

Interfacial phase competition induced Kondo-like effect in manganite-insulator composites

Ling-Fang Lin¹, Ling-Zhi Wu², Shuai Dong^{1,†}

¹*Department of Physics, Southeast University, Nanjing 211189, China*

²*School of Geography and Biological Information,
Nanjing University of Posts and Telecommunications, Nanjing 210046, China*

Corresponding author. E-mail: †sdong@seu.edu.cn

Received February 26, 2016; accepted March 31, 2016

A Kondo-like effect, namely, the upturn of resistivity at low temperatures, is observed in perovskite manganite when nonmagnetic insulators are doped as secondary phase. In this paper, the low-temperature resistivity upturn effect has been argued to originate from interfacial magnetic phase reconstruction. Heisenberg spin lattices have been simulated using the Monte Carlo method to reveal phase competition around secondary phase boundary, namely, manganite-insulator boundary that behaves with a weak antiferromagnetic tendency. Moreover, the resistor network model based on double-exchange conductive mechanism reproduces the low-temperature resistivity upturn effect. Our work provides a reasonable physical mechanism to understand the novel transport behaviors in microstructures of correlated electron systems.

Keywords manganite, Kondo-like effect, manganite-insulator composites, phase competition

PACS numbers 75.47.Lx, 75.47.Gk, 73.63.-b

1 Introduction

Perovskite oxides are typical correlated electron systems and important functional materials, owning fascinating physical properties and promising potential for applications [1–3]. As a typical perovskite family, manganites have attracted considerable attention because of their strongly correlated electron characteristics, especially the colossal magnetoresistance (CMR) effect [2, 3]. The physical properties of manganites sensitively depend on the spin and charge/orbital orders. Moreover, competitions between various phases that have close free energies but divergent physical properties are responsible for the CMR effect [4–6]. Despite the colossal effect, the CMR has not been successfully used in applications to replace the giant magnetoresistance effect observed in magnetic metal multilayers. An important bottleneck of the CMR is that it requires large magnetic fields, usually on the order of 1 T [3], which is difficult to realize in microdevices.

To overcome this drawback, in recent years, researchers have studied various manganite-insulator composites to improve low-field magnetoresistance [7, 8]. With insulators embedded in a wide-bandwidth manganite like $\text{La}_{2/3}\text{Sr}_{1/3}\text{MnO}_3$, prominent magnetoresistance can be realized with relatively low magnetic fields. Not only enhanced low-field magnetoresistance but also the Kondo-like effect, namely, upturn of resistivity at low temperatures, has been observed when nonmag-

netic insulators as a secondary phase were doped into $\text{La}_{2/3}\text{Sr}_{1/3}\text{MnO}_3$ [7, 9, 10]. Originally, Kondo effect was used to describe a change in the characteristic electrical resistivity with temperature of a metal that results from the scattering of conduction electrons off magnetic impurities [11].

However, the Kondo-like effect observed in manganite-insulator composites is somewhat different from the conventional Kondo effect for the following reasons. First, the carriers in manganite are spin-polarized and, unlike the magnetic impurities in the Kondo effect, the nonmagnetic insulators cannot play the role of a magnetic scatter center. Second, the scale of the nonmagnetic cluster here is on the micrometer scale, which is much larger than the mean free path of the electrons in manganite and drastically different from the atomic-scale impurities in metal alloys. Extensive experimental and theoretical works [12–15] have been performed over the past years, and several mechanisms have been proposed to interpret the resistivity minima observed in manganite-insulator composites, most of which are still under debate. A clear and widely accepted physical scenario remains absent.

The double-exchange model proposed by Zener and a strong electron-phonon interaction deriving from the Jahn–Teller splitting of Mn $3d$ levels can explain many of the electrical and magnetic properties of manganite. However, such a quantum model cannot be directly applied to describe the transport phenomena on the mi-

rometer scale. Therefore, the origin of the resistivity minima observed in manganite-insulator composites has not been completely understood [16–18].

In this article, we propose a new physical scenario based on interfacial phase competition as the origin of the Kondo-like resistivity upturn effect. Previous studies have shown that because of the inherent phase competition between the ferromagnetic phase and charge-ordered antiferromagnetic phase [1], the ferromagnetism of manganites can be significantly suppressed in the interfacial layers contacting insulators [19]. Meanwhile, the secondary phase boundary can lead to a weak antiferromagnetic tendency [19]. Moreover, the transport properties of such phase competing interfaces have not been theoretically investigated.

2 Model and methods

In the current work, the double-exchange conductance is calculated using classical resistor networks for a Heisenberg spin model to reveal the fascinating Kondo-like effect in manganite-insulator composites. First, the Heisenberg spin model is a general model for magnetic systems and can be applied to describe the magnetic transition in $\text{La}_{2/3}\text{Sr}_{1/3}\text{MnO}_3$. Second, the resistor network method has been successfully adopted to simulate the transport in manganite. It can handle a large-scale system without losing the double-exchange feature [20–25].

In our model, as shown in Fig. 1, an isolated cluster of insulators (region III) is embedded in the magnetic manganite background (region I) as a secondary phase. Because of the interfacial reconstruction, such as the change of local electron concentration or strains, the manganite-insulator boundary (region II) behaves with a weak antiferromagnetic (AFM) tendency and has a lower critical temperature than the pristine ferromagnetic (FM) Curie temperature of the manganite [19].

The Heisenberg spin model on a two-dimensional (2D) square lattice ($L \times L$, $L = 31$ here) with periodic boundary conditions is adopted in the following simulation. The Hamiltonian of the Heisenberg spin lattice model reads

$$H = - \sum_{\langle i,j \rangle} J_{i,j} S_i \cdot S_j - S_i \cdot h, \quad (1)$$

where $J_{i,j}$ is the exchange interaction between the nearest-neighbor (NN) spins S_i and S_j , h is the external magnetic field, and the length of spin is normalized as unity. As shown in Fig. 1, the exchange interaction J_I in region I is uniformly positive for the FM manganite, which is taken as the energy unit for simplicity. For the interfacial region, the exchange interaction J_{II} is negative for a weak AFM coupling, and its absolute value is smaller than J_I .

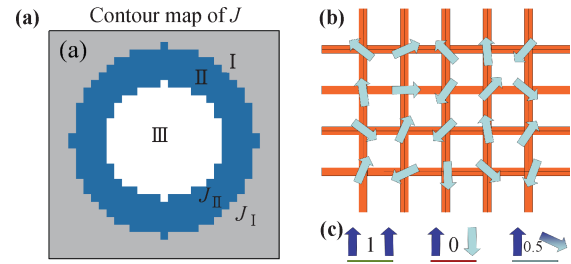


Fig. 1 (a) Schematic diagram of the contour map of J on the 2D spin lattices. Regions I, II, and III represent the manganite background, manganite-insulator boundary, and insulating impurity cluster, respectively. (b) Schematic diagram of the network resistor of the Heisenberg spin lattice with periodic boundary conditions. The arrow on each site represents spin. The orange frame connecting every NN sites is the resistor network. (c) Sketch of the local resistor calculated based on the double-exchange process between the NN spins pair. Left: When adjacent spins are parallel, the local conductance is the maximum value of 1. Middle: When the NN spins are antiparallel, the local conductance is 0. Right: For an arbitrary angle between the NN spins pair, for example 120° , the local conductance can be calculated using Eq. (2).

The standard Markov chain Monte Carlo (MC) method with the Metropolis algorithm is employed to study the temperature-dependent properties of the lattice. In our MC simulation, the spin lattice is initialized randomly. Then, the first 1×10^4 MC steps (MCSs) are used for thermal equilibrium, and the remaining 1×10^4 MCSs are used for measurements. In all simulations, the acceptance ratio of MC updates is well controlled at approximately 50% by adjusting the updating windows for the spin vectors, which can give rise to the most efficient MC sampling [26].

In each MC measurement, a resistor network is built based on the spin lattice and the total resistance of the system is calculated [22–25]. As show in Fig. 2, a resistor is assigned between each NN site pair with the value

$$C_{i,j} = \sqrt{(1 + S_i \cdot S_j)/2}. \quad (2)$$

This formula can be used to describe a spin-dependent double-exchange process. The physical meaning is that when adjacent spins are parallel, the conductance is maximum, and conversely, when the NN spins are antiparallel, the conductance is forbidden. Between these two limits, the conductance is determined by the spin angle according to the double-exchange formula [27]. The conductance between the regions I and II is set to be 0, and so is in region I. The whole resistor network is solved using Kirchhoff's equations. Specifically, a system of linear Kirchhoff's equations is constructed for each site and reads

$$\sum_j C_{i,j} (V_i - V_j) = 0, \quad (3)$$

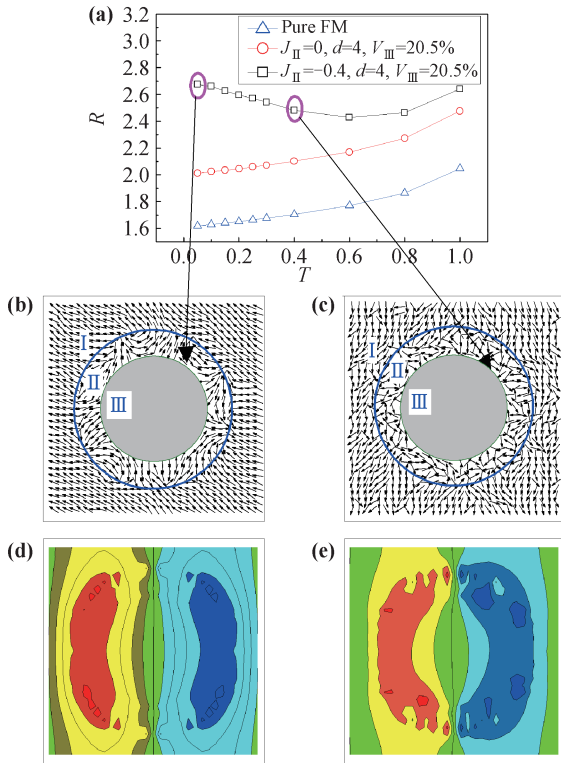


Fig. 2 (a) MC results of the temperature dependence of the resistance for the cases: (1) $J_{II} = J_I = 1$, a pure FM lattice; (2) $J_{II} = 0$, the one with disordered interfacial layers; (3) $J_{II} = -0.4$, the regular one with an interfacial AFM coupling. (b, c) Snapshots of the 2D spin patterns at $T = 0.05$ and $T = 0.4$, respectively, corresponding to the circles in Fig. 2(a). (d, e) Contour maps for the potential difference of the whole resistor network: (d) comparison between (i) the pure FM lattice and (ii) the regular one at $T = 0.05$; (e) comparison between (i) $T = 0.05$ and (ii) $T = 0.4$ for the identical regular lattice.

where V_i and V_j are the voltages at the NN sites i and j , respectively, and $C_{i,j}$ is the conductance of the local resistor between sites i and j calculated using Eq. (2).

It should be noted that although the resistor network has been used to study the percolation in phase-separated manganites, the present model goes beyond the previous studies [22–25]. Previously, two or three types of fixed resistors were used to construct the network, which could not simulate the interfacial effect in region II. Only after considering the detailed correlation between the Heisenberg spins, as done in the current work, the model can handle the spin-dependent transport in such manganite-insulator composites.

3 Results and discussion

First, the temperature dependence of the resistance is compared between the pure FM bulk (with region III

but without region II) and the one with an interfacial region (i.e., region II), as shown in Fig. 2(a). For the pure FM bulk, the resistance–temperature (R – T) curve displays a good metallic behavior, i.e., the resistance decreases in the cooling progress, even when an insulator embedded in the lattice. When the interfacial region is taken into account, the upturn of resistivity indeed shows up clearly at low temperatures, and the minimum resistance appears at $T = 0.6$ when the doping concentration is 20.5%, characterized by the volume of region III (V_{III}). In the above simulation, the weak exchange interaction in region II is $J_{II} = -0.4$ and the thickness of region II is $d = 4$. To further understand the underlying mechanism, one more simulation is performed by setting J_{II} as 0 and keeping all the other parameters unchanged. In this case, the spins in region II are always in random directions (i.e., paramagnetic), and the upturn resistivity effect disappears, as shown in Fig. 2(a). The above comparisons imply the key role of the AFM coupling in the interfacial region in the Kondo-like resistivity upturn.

To understand the relationship between magnetism and transport behavior, two MC snapshots of the spin lattice at $T = 0.05$ and $T = 0.4$ are shown in Figs. 2(b) and (c), respectively. In both cases, the lattice displays a robust FM order in region I. In region II, the spins are somewhat “disordered” at $T = 0.4$, and the “disordered” pattern gradually turns to be an AFM-ordered at low temperatures.

The direct relationship between the magnetic transition and upturn of the resistance can be intuitively visualized by the profiles of electrical potential differences. Figure 2(d) shows the contour map for the potential difference of the whole resistor network between the pure FM lattice and the one with region II at $T = 0.05$. Similarly, Fig. 2(e) shows the potential difference at $T = 0.05$ and $T = 0.4$ for the same lattice with region II. In both contour maps, there is a distinct difference in the region surrounding the embedded insulator cluster, namely, the interface layers between the manganite and insulator materials.

As a summary of Fig. 2, the manganite matrix, which changes from the paramagnetic to FM order with decreasing temperature, exhibits a metallic transport behavior. Then, the AFM phase transition in region II is responsible for the resistivity upturn at low temperatures considering the double-exchange process presented in Eq. (2).

The above simulations a possible physical process that induces the Kondo-like resistivity upturn effect. The magnetic field and temperature dependence of the resistivity was systematically simulated as follows. First, the different doping concentrations were simulated by changing the relative volume V_{III} for a fixed thickness of region II ($d = 5$) and a weak exchange interaction in region II ($J_{II} = -0.4$). As shown in Fig. 3(a), the upturn amplitude of the resistance is more prominent

with increasing V_{III} , while the temperature at which the resistance develops a minimum (denoted by T_{min}) almost does not shift. This is reasonable because the interfacial perimeter (and thus the volume of region II) increases linearly with the radius of the embedded insulator. Second, by fixing the values of d and V_{III} , the temperature of minimum resistance shows an increasing tendency with the absolute value of J_{II} , as displayed in Fig. 3(b). The reason being simply because a strong J_{II} corresponds to a high AFM transition temperature, even though the amplitude of the upturn appears to be strong in the weak $|J_{\text{II}}|$ case. Third, Fig. 3(c) shows the changes in the R - T curves with increasing thickness of region II while the other parameters are fixed. The value of T_{min} is almost unchanged while the upturn amplitude is significantly enhanced in the large d case. Last, we switch on the external magnetic field and study the magnetoresistance effect. As shown in Fig. 3(d), it is evident that the applied magnetic field suppresses the upturn effect. The value of T_{min} gradually decreases with increasing magnetic field, and finally, the system turns to be a full metal. This process can be understood as the suppression of the weak AFM correlation in region II by magnetic fields, which polarize all spins parallel, and thus, the whole FM correlation is established in regions I and II. In our simplified model, T_{min} corresponds to the interfacial magnetic phase transition, which is determined by the strength of the exchange interactions J_2 and external magnetic field h . Therefore, T_{min} is almost unchanged as d increases; however, it can be shifted by the applied magnetic field.

Our results point out that the low-temperature resistivity upturn can be tuned by the interfacial parameters

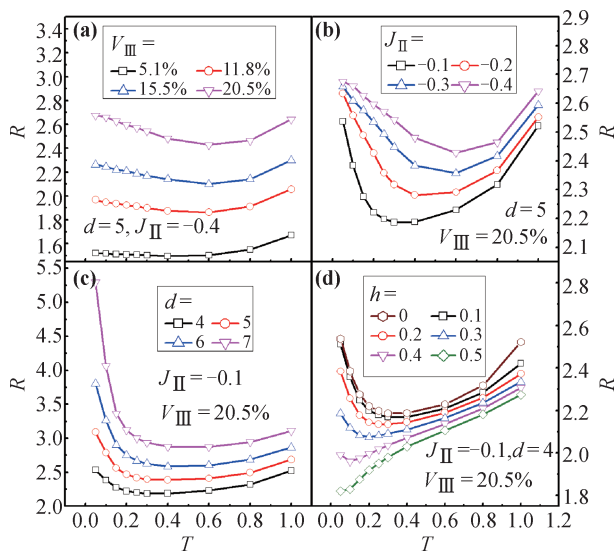


Fig. 3 MC results of resistance as a function of temperature for various values of (a) doping concentration characterized by the volume of insulator cluster, (b) exchange interaction in region II, (c) thickness of region II, and (d) external magnetic field.

as well as external magnetic fields. The amplitude of the upturn and the value of T_{min} depend on various physical factors. Our study can help researchers to fine-tune the Kondo-like effect in future experiments.

4 Summary

In conclusion, Monte Carlo simulations were performed on the Heisenberg spin lattices and resistor network model to qualitatively investigate the low-temperature resistivity upturn effect in manganite-insulator composites. The resistor network was constructed based on the spin-dependent double-exchange process. The temperature dependence of the resistivity at different conditions was systematically simulated. Our simulation found that the antiferromagnetic tendency of the manganite-insulator boundary due to interfacial reconstruction leads to the low-temperature resistivity upturn effect. Our toy model provided a simple yet intuitive physical picture to clarify a possible mechanism of the Kondo-like transport behavior in correlated electronic materials.

Acknowledgements We thank G. X. Cao, Y. Z. Gao, and Y. K. Tang for helpful discussions. This work was supported by the National Natural Science Foundation of China (Grant Nos. 11274060 and 51322206).

References

1. H. M. Zhang, M. An, X. Y. Yao, and S. Dong, Orientation-dependent ferroelectricity of strained PbTiO_3 films, *Front. Phys.* 10(6), 107701 (2015)
2. E. Dagotto, T. Hotta, and A. Moreo, Colossal magnetoresistant materials: The key role of phase separation, *Phys. Rep.* 344(1), 1 (2001)
3. Y. Tokura, Critical features of colossal magnetoresistive manganites, *Rep. Prog. Phys.* 69(3), 797 (2006)
4. C. Şen, G. Alvarez, and E. Dagotto, Competing ferromagnetic and charge-ordered states in models for manganites: The origin of the colossal magnetoresistance effect, *Phys. Rev. Lett.* 98(12), 127202 (2007)
5. C. Şen, G. Alvarez, and E. Dagotto, First order colossal magnetoresistance transitions in the two-orbital model for manganites, *Phys. Rev. Lett.* 105(9), 097203 (2010)
6. M. An, H. M. Zhang, Y. K. Weng, Y. Zhang, and S. Dong, Possible ferrimagnetism and ferroelectricity of half-substituted rare-earth titanate: A first-principles study on $\text{Y}_{0.5}\text{La}_{0.5}\text{TiO}_3$, *Front. Phys.* 11(2), 117501 (2016)
7. M. Staruch, H. Gao, P. X. Gao, and M. Jain, Low-field magnetoresistance in $\text{La}_{0.67}\text{Sr}_{0.33}\text{MnO}_3$: ZnO composite film, *Adv. Func. Mater.* 22(17), 3591 (2012)
8. Y. K. Tang, X. F. Ge, X. F. Si, W. J. Zhao, Y. Wang, S.

- Dong, Y. Zhai, Y. Sui, W. H. Su, and C. C. Almasan, Influence of magnetic correlations on low-field magnetoresistance in $\text{La}_{2/3}\text{Sr}_{1/3}\text{MnO}_3/\text{SrTiO}_3$ composites, *Phys. Status Solidi A* 210(6), 1195 (2013)
9. Y. Gao, G. X. Cao, J. Zhang, and H. U. Habermeier, Intrinsic and precipitate-induced quantum corrections to conductivity in $\text{La}_{2/3}\text{Sr}_{1/3}\text{MnO}_3$ thin films, *Phys. Rev. B* 85(19), 195128 (2012)
 10. G. X. Cao, J. C. Zhang, S. X. Cao, C. Jing, and X. C. Shen, Magnetization step, history-dependence, and possible spin quantum transition in $\text{Pr}_{5/8}\text{Ca}_{3/8}\text{MnO}_3$, *Phys. Rev. B* 71(17), 174414 (2005)
 11. J. Kondo, Resistance minimum in dilute magnetic alloys, *Prog. Theor. Phys.* 32(1), 37 (1964)
 12. E. Rozenberg, M. Auslender, I. Felner, and G. Gorodetsky, Low-temperature resistivity minimum in ceramic manganites, *J. Appl. Phys.* 88, 2578 (2000)
 13. T. A. Costi, Kondo effect in a magnetic field and the magnetoresistivity of Kondo alloys, *Phys. Rev. Lett.* 85(7), 1504 (2000)
 14. J. Zhang, Y. Xu, L. Yu, S. Cao, and Y. Zhao, Resistivity minimum and the electronic strongly correlation characteristic for $\text{La}_{2/3}\text{Sr}_{1/3}\text{MnO}_3$ thin film, *Physica B* 403(5), 1471 (2008)
 15. Y. Matsushita, H. Bluhm, T. H. Geballe, and I. R. Fisher, Evidence for charge Kondo effect in superconducting Tl-doped PbTe, *Phys. Rev. Lett.* 94(15), 157002 (2005)
 16. M. Ziese, Searching for quantum interference effects in $\text{La}_{0.7}\text{Ca}_{0.3}\text{MnO}_3$ films on SrTiO_3 , *Phys. Rev. B* 68(13), 132411 (2003)
 17. D. Kumar, J. Sankar, J. Narayan, R. K. Singh, and A. K. Majumdar, Low-temperature resistivity minima in colossal magnetoresistive $\text{La}_{0.7}\text{Ca}_{0.3}\text{MnO}_3$ thin films, *Phys. Rev. B* 65(9), 094407 (2002)
 18. E. Syskakis, G. Choudalakis, and C. Papastaikoudis, Crossover between Kondo and electron–electron interaction effects in $\text{La}_{0.75}\text{Sr}_{0.20}\text{MnO}_3$ manganite doped with Co impurities? *J. Phys.: Condens. Matter* 15(12), 7735 (2003)
 19. L. Brey, Electronic phase separation in manganite-insulator interfaces, *Phys. Rev. B* 75(10), 104423 (2007)
 20. H. W. Guo, J. H. Noh, S. Dong, P. D. Rack, Z. Gai, X. S. Xu, E. Dagotto, J. Shen, and T. Z. Ward, Electrophoretic-like gating used to control metal-insulator transitions in electronically phase separated manganite Wires, *Nano Lett.* 13(8), 3749 (2013)
 21. W. G. Wei, Y. Y. Zhu, Y. Bai, H. Liu, K. Du, K. Zhang, Y. F. Kou, J. Shao, W. B. Wang, D. L. Hou, S. Dong, L. F. Yin, and J. Shen, Direct observation of current-induced conductive path in colossal-electroresistance manganites thin films, *Phys. Rev. B* 93, 035111 (2016)
 22. S. Dong, H. Zhu, X. Wu, and J. M. Liu, Microscopic simulation of the percolation of manganites, *Appl. Phys. Lett.* 86(2), 022501 (2005)
 23. S. Dong, H. Zhu, and J. M. Liu, Dielectrophoresis model for the colossal electroresistance of phase-separated manganites, *Phys. Rev. B* 76(13), 132409 (2007)
 24. S. Ju, T. Y. Cai, and Z. Y. Li, Percolative magnetotransport and enhanced intergranular magnetoresistance in a correlated resistor network, *Phys. Rev. B* 72(18), 184413 (2005)
 25. L. F. Lin, X. Huang, and S. Dong, Simulation of the magnetoresistance of Heisenberg spin lattices using the resistor-network model, *Chin. Phys. B* 22(11), 117313 (2013)
 26. D. P. Landau and K. Binder, A Guide to Monte Carlo Simulations in Statistical Physics, Ed. 3, Cambridge: Cambridge University Press, 2014
 27. S. H. Tsai and D. P. Landau, Simulations of a classical spin system with competing superexchange and double-exchange interactions, *J. Appl. Phys.* 87(9), 5807 (2000)